Two superimposed cold and fresh anomalies enhanced Irminger Sea deep convection in 2016 – 2018

Patricia ZUNINO [1], Herlé MERCIER [2], Virginie THIERRY [3]

[1] Altran Technologies, Technopôle Brest Iroise, Site du Vernis , 300 rue Pierre Rivoalon, 29200 Brest, France,
[2] CNRS, University of Brest, IRD, Ifremer, Laboratoire d'Océanographie Physique et Spatiale (LOPS), IUEM, ZI de la pointe du diable, CS 10070 - 29280 Plouzané, France
[3] Ifremer, University of Brest, CNRS, IRD, Laboratoire d'Océanographie Physique et Spatiale (LOPS), IUEM, ZI de la pointe du diable, CS 10070 - 29280 Plouzané, France

CONTACT: patricia.zuninorodriguez@altran.com

1. Introduction

Deep convection is the result of a process by which surface waters loose buoyancy and sink into the interior ocean. It occurs only where specific conditions are met including large air-sea buoyancy loss and favorable preconditioning (Marshall & Schott, 1999). In the Subpolar North Atlantic (SPNA), it takes place in the Labrador Sea and in the Irminger Sea.
While Earth system models project a reduction, or even a shut-down, of deep convection in the North Atlantic Ocean in response to anthropogenic forcing, deep convection returned to the Irminger Sea in 2008 and occurred several times since then to reach exceptional depths > 1,500 m in 2015 and 2016.
The objectives of this work are:

- To continue the monitoring of deep convection in the Irminger Sea
- To identify the causes of the increase in the depth of the convection
- Because the expected increase in the freshwater inputs in the SPNA (Bamber et al., 2018), to reveal the role of salinity in inhibiting or enhancing the deep convection .

2. Data and Methods

The atmospheric forcing was evaluated using ERA-Interim reanalysis (Dee et al., 2011) and EN4 data (Good et al., 2013) as:

i) the air-sea buoyancy flux (B_{surf})

$$B_{surf} = \frac{\alpha.g}{\rho_0.c_p}.Q - \beta.g.SSS.FWF \qquad \text{Eq. 1}$$

i) the horizontal Ekman buoyancy flux (Bf_{ek})

$$BF_{ek} = -g.(U_e\partial_x SSD + V_e\partial_y SSD).\frac{C_p}{\alpha.g} \qquad \text{Eq. 2}$$

The preconditioning was evaluated as Buoyancy that has to be removed ($B(zi)$) from the late summer water column to homogenize it down to a depth *zi* (eq. 3, Schmidt and Send, 2007), using September Argo data http://www.argo.ucsd.edu/, http://www.coriolis.eu.org/).

$$B(zi) = \frac{g}{\rho_0} * \sigma_0(zi) * zi - \frac{g}{\rho_0}\int_{zi}^{o}\sigma_0(z)dz \qquad \text{Eq. 3}$$

We split B into a temperature (B_θ) and salinity (B_S) term as:

$$B_\theta(zi) = -(g * \alpha * \theta(zi) * zi - g * \alpha * \int_{zi}^{o}\theta(z)\,dz) \qquad \text{Eq. 4}$$

$$B_S(zi) = g * \beta * S(zi) * zi - g * \beta * \int_{zi}^{o}S(z)dz \qquad \text{Eq. 5}$$

3. Results

3.1 Deep convection in Irminger Sea in Winters 2017 and 2018

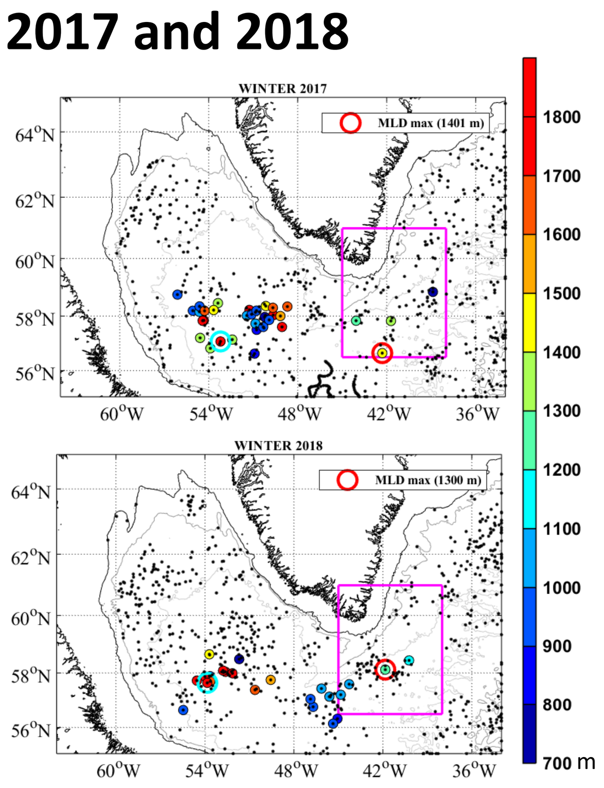

Figure 1. Position of all Argo floats between 1 January and 30 April 2017 and 2018 (small black points). The colored big points and colorbar indicate the depth of the mixed layer depth (MLD), MLD deeper than 700 m indicates deep convection. The circles correspond to the positions of the profiles with the maximum MLD. The pink box delimit the regions used for estimating the time series of atmospheric forcing and the vertical profiles of buoyancy to be removed in the Irminger Sea (56.5°N – 61.0°N and 45.0°W – 38.0°W).

3.2 Atmospheric Forcing

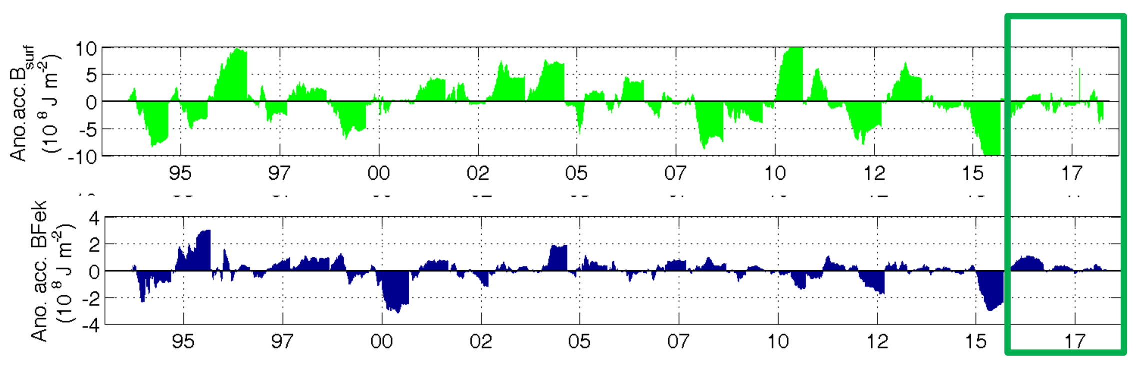

Figure 2. Time series of anomalies of accumulated air-sea buoyancy flux (B_{surf}*) and horizontal Ekman buoyancy flux (BF_{ek}), averaged in the Irminger Sea (pink box in Fig. 1). They are anomalies with respect to 1993 – 2016. The accumulation was from 1 September to 31 August the following year.

3.3 Preconditioning of the water column

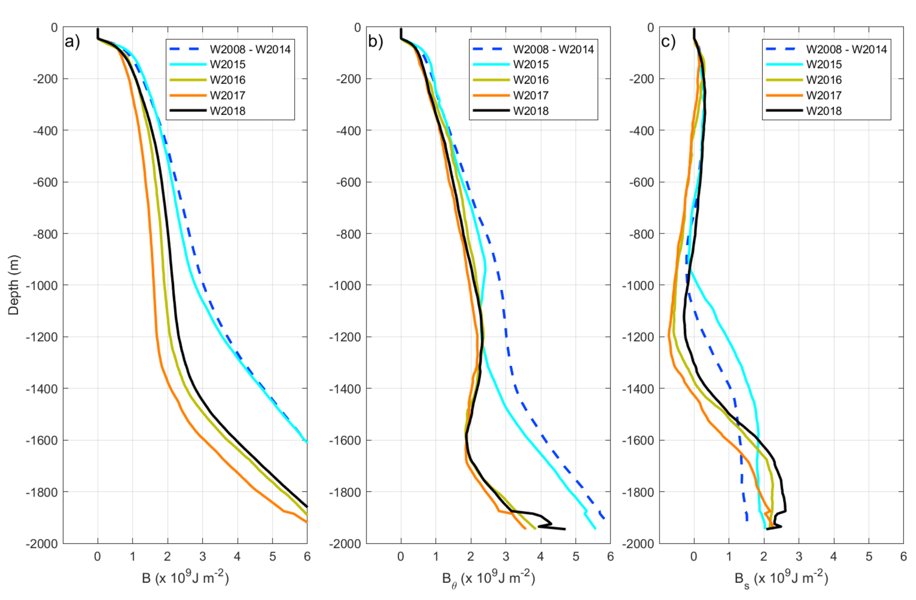

Figure 3. Vertical profile of a) the total buoyancy to be removed (**B**), b) the thermal component (**B_θ**) and c) the salinity component (**B_s**). They were calculated from Argo data measured in the Irminger box (see Fig. 1) in September before the winter indicated in the legend.

3.4 Origin of the favorable preconditioning of the water column

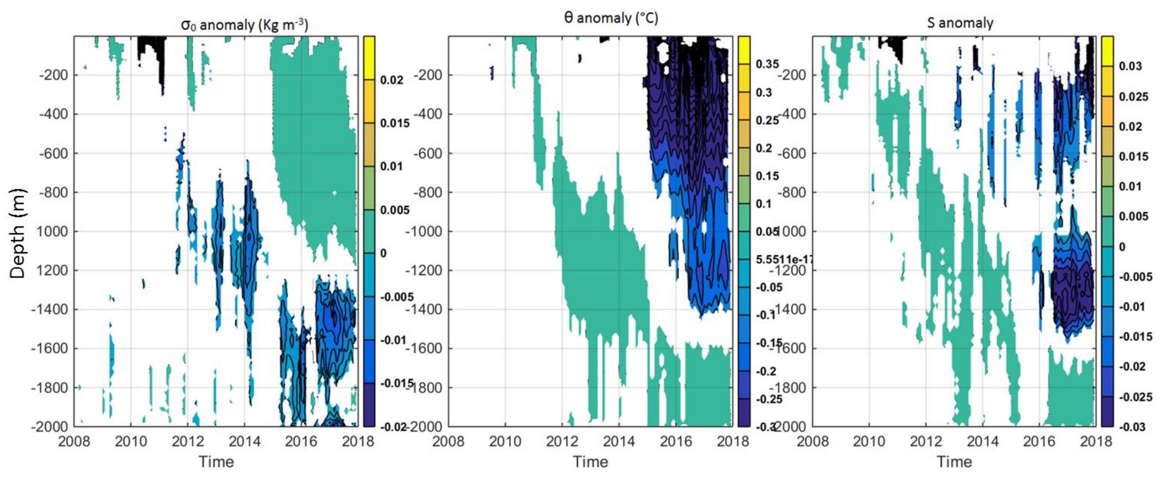

Figure 4. Evolution of vertical profiles of monthly anomalies of σ_0, θ and S, at 59°N, 40°W in the Irminger Sea. Data source: ISAS database (Kolodziejczyk et al., 2017). Anomalies referenced to the monthly mean estimated for 2002 – 2016. We represented only anomalies larger than one standard deviation.

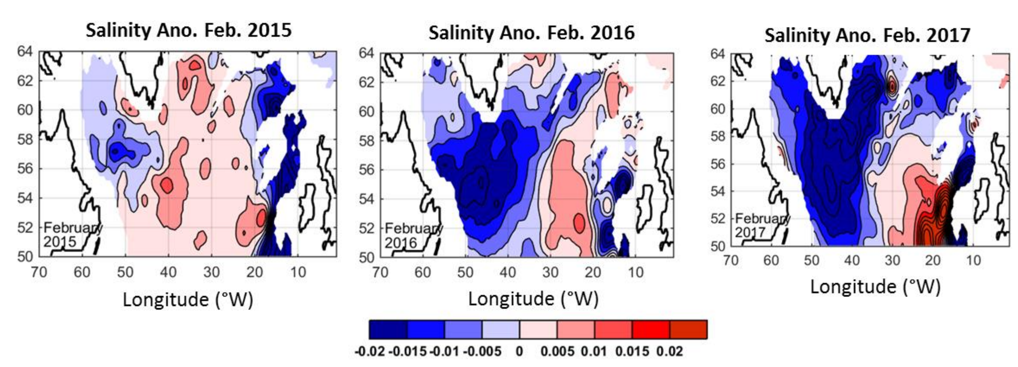

Figure 5. Horizontal distribution of the anomalies of S in the layer 1200 – 1400 m in February 2015, February 2016 and February 2017. The monthly anomalies were estimated from ISAS database referenced to the period 2002 – 2016.

3.5 Comparison of preconditioning in Irminger Sea and Labrador Sea

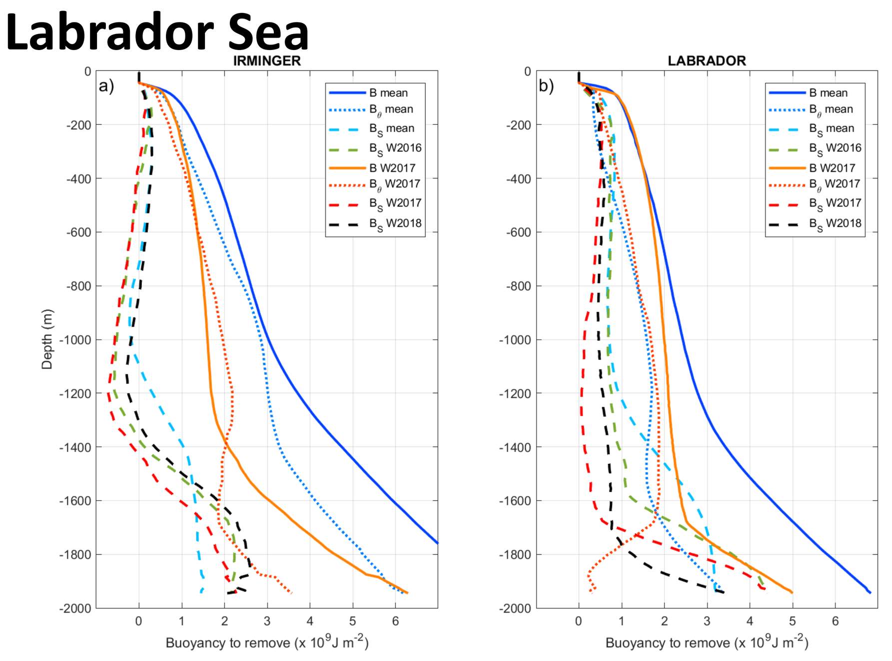

Figure 6. Decomposition of profiles of B (continuous lines) in B_θ (point lines) and B_s (discontinuous lines) in a) the Irminger Sea; b) the Labrador Sea. To compare the mean 2008 – 2014 with W2017 compare reddish lines with bluish lines. The B_s component in W2016 and W2018 was added in order to show the evolution of the depth of the deep halocline in both the Irminger Sea and the Labrador Sea.

4. Conclusion

- Deep convection deeper than 1,300 m occurred in the Irminger Sea during 2016 – 2018. It was possible because the favorable preconditioning of the water column since the atmospheric forcing was close to the mean.
- The cooling of the intermediate water was essential to reach convection depth of ~800 – 1,000 m, and the freshening in the layer 1,200 – 1,400 m and the associated deepening of the deep halocline, allowed the very deep convection during winters 2016 – 2018.
- The cooling of the layer 200 – 800 m likely originated locally during W2015 when extraordinary deep convection happened. The freshening of the layer 1,200 – 1,400 m appeared in 2016 and given its depth range, it is unlikely that this anomaly was locally formed, it was rather advected from the Labrador Sea.
- By working with B profiles and splitting it in its thermal and salinity terms we show: i) B_θ governs B in the upper 1,000 m and ii) B_s importantly increase B in the layer 1,000 – 1,400 m, which indicates that the deep halocline (LSW - ISOW) likely limits the depth of the convection in the Irminger Sea.

References

Bamber, J. L., et al.: Land Ice Freshwater Budget of the Arctic and North Atlantic Oceans: 1. Data, Methods, and Results, *Journal of Geophysical Research: Oceans*, 1–11, https://doi.org/10.1002/2017JC013605, 2018.

Dee, D. P.,et al.: The ERA-Interim reanalysis: Configuration and performance of the data assimilation system, *Quarterly Journal of the Royal Meteorological Society*, *137*(656), 553–597. https://doi.org/10.1002/qj.828, 2011.

Good, S. A., et al.: EN4: Quality controlled ocean temperature and salinity profiles and monthly objective analyses with uncertainty estimates. *J. of Geoph. Research: Oceans*, *118*(12), 6704–6716. https://doi.org/10.1002/2013JC009067, 2013.

Kolodziejczyk, N. et al. : ISAS-15 temperature and salinity gridded fields. SEANOE. http://doi.org/10.17882/52367, 2017.

Marshall, J., & Schott, F.: Open-Ocean Convection ' Theory , and Models Observations ,. *Reviews of Geophysics*, *37*(98), 1–64. https://doi.org/10.1029/98RG02739, 1999.

Schmidt, S., & Send, U.: Origin and Composition of Seasonal Labrador Sea Freshwater, *Journal of Physical Oceanography*, *37*(6), 1445–1454. https://doi.org/10.1175/JPO3065.1, 2007.

Zunino et al.: Two superimposed cold and fresh anomalies enhanced Irminger Sea deep convection in 2016 – 2018. Ocean Science. https://www.ocean-sci-discuss.net/os-2019-40/